Physics Letters A 374 (2010) 3671–3675

Contents lists available at ScienceDirect

Physics Letters A

www.elsevier.com/locate/pla

# First-principles study on ferromagnetism in C-doped AlN

Kai Li [a], Xiaobo Du [a], Yu Yan [a,*], Hongxia Wang [b], Qing Zhan [c], Hanmin Jin [a]

[a] State Key Laboratory of Superhard Materials and Department of Physics, Jilin University, Changchun, 130021, PR China
[b] College of Mathematics, Physics and Information Science, Zhejiang Ocean University, Zhoushan, 316000, PR China
[c] Jilin Provincial Institute of Education, Changchun, 130022, PR China

ARTICLE INFO

*Article history:*
Received 13 April 2010
Received in revised form 28 June 2010
Accepted 6 July 2010
Available online 13 July 2010
Communicated by R. Wu

*Keywords:*
C-doped AlN
Ferromagnetism
First-principles

ABSTRACT

First-principles calculations are performed to study the electronic structures and magnetic properties of C-doped AlN. Both generalized gradient approximation (GGA) and GGA + $U$ calculations show that a substitutional C atom introduces magnetic moment of about 1.0 $\mu_B$, which comes from the partially occupied 2p orbitals of the C, its first neighboring Al and first neighboring N atoms (GGA) or out-of-plane first and fifth neighboring N atoms (GGA + $U$), among which the atomic moment of the C is the biggest. The $U$ correction for the anion-2p states obviously changes the magnetic moment distribution of Al and N atoms and transforms the ground state of C-doped AlN to insulating from half-metallic. The C atoms can induce ferromagnetic ground state with long-range couplings between the moments in C-doped AlN. The ferromagnetic coupling can be explained in terms of the two band coupling model.



## 1. Introduction

Diluted magnetic semiconductors (DMS) have attracted much attention for their potential applications in the field of spintronics. Such applications require the DMS to be ferromagnetic above room temperature. High-temperature ferromagnetism has been reported by many researchers in several types of transition-metal (TM)-doped semiconducting oxides and nitrides [1–6]. However, the origin of the ferromagnetism observed in TM-doped semiconductors is still under debate. It was found that the magnetic TM dopants in TM-doped DMS segregate to form ferromagnetic clusters, precipitates or secondary phases [7–9], which are obstacles for the practical applications of DMS. To avoid these extrinsic magnetic behaviors, many researches have been focused on investigating the effect of nonmagnetic ion doping in semiconductors to obtain high temperature ferromagnetic semiconductors based on nonmagnetic ion dopants. Besides the discovery of ferromagnetism in nonmagnetic cation doped semiconductors, the experimental researches demonstrated that high temperature ferromagnetism also can be obtained in nonmagnetic anion C- and N-doped ZnO and $TiO_2$ and C-doped GaN [10–19]. Furthermore, first-principles calculations reported that anion C or N substitutions in several oxides, sulfides and nitrides can induce ferromagnetism and the ferromagnetism is intrinsic [18–34].

AlN is one of the most promising semiconductors for optoelectronic devices, and realization of high temperature ferromagnetism in TM-doped AlN makes it attractive for multifunctional devices. It has been reported that nonmagnetic cation Cu- and Sc-doped AlN are ferromagnetic at temperatures above 300 K [35–37]. Due to the frequent usage of C as dopant of III–V nitrides, many works have been made to study the structural and electronic properties and the formation energies of substitutional C impurities in AlN [38–42]. So far, there has not been a detailed report on the magnetic properties of nonmagnetic anion C-doped AlN. In order to explore possible magnetic properties of C-doped AlN, we investigate the effects of nonmagnetic C dopants on the electronic structures and magnetic properties of C-doped AlN by first principles calculations.

## 2. Computational details

The calculations were performed using Vienna ab-initio simulation package (VASP) [43,44]. The exchange–correlation potential was treated with the generalized gradient approximation (GGA) [45] and the strong correlation effects were introduced by means of GGA + $U$ scheme [46]. It has been known that electronic correlation effects are important for the structural, electronic and magnetic properties of systems involving localized 2p orbitals of first-row anions, and inclusion of the correlation effects for the anion-2p electrons by means of the local spin-density approximation (LSDA) + $U$ or GGA + $U$ scheme can give improved results [31–33]. For the GGA + $U$ calculations, the on-site Coulomb and exchange parameter for anion-2p states was taken as $U = 5.6$ eV and $J = 1.2$ eV, respectively, which is almost the same as the value used in Refs. [31] and [32] and is close to the estimated values from spectroscopic measurements in oxides [47–49]. The electron–ion interaction was described by the projector augmented wave method. The electronic wave function was expanded in plane wave

* Corresponding author. Tel.: +86 0431 88499047.
*E-mail address:* yanyu@jlu.edu.cn (Y. Yan).

0375-9601/$ – see front matter 
doi:10.1016/j.physleta.2010.07.011

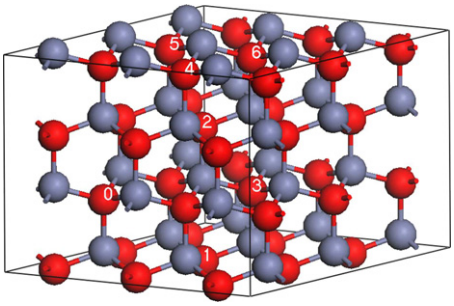


**Fig. 1.** (Color online.) 72-atom $3 \times 3 \times 2$ supercell of AlN. The red and gray balls represent N and Al atoms, respectively. The positions of N substituted by C are denoted by 0–6.

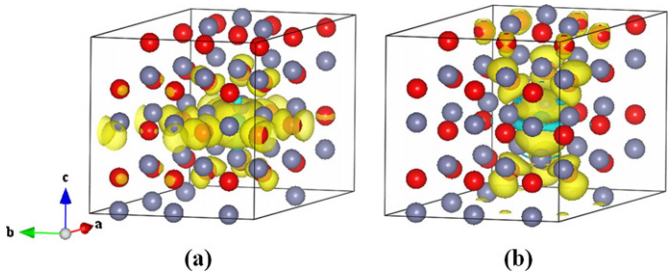


**Fig. 2.** (Color online.) The spin density distribution in the relaxed $3 \times 3 \times 2$ supercell containing a substitutional C atom calculated by GGA (a) and GGA + $U$ (b). The yellow and blue isosurfaces correspond to the majority- and minority-spin densities. The red, gray and green balls represent N, Al and C atoms, respectively.

**Table 1**
The magnetic moments of the C atom ($M_C$), its four nearest neighboring Al atoms ($M_{Al}$) and all of N atoms ($M_N$).

| | $M_C$ ($\mu_B$) | $M_{Al}$ ($\mu_B$) | $M_N$ ($\mu_B$) |
|---|---|---|---|
| GGA | 0.276 | 0.043 | 0.231 |
| GGA + $U$ | 0.280 | 0.041 | 0.250 |

up to a cutoff energy of 400 eV, and a $5 \times 5 \times 3$ Monkhorst–Pack k-point grid was used to sample the Brillouin zone.

AlN crystallizes in the hexagonal wurtzite phase under ambient conditions. The C-doped AlN system was modeled with a supercell built of $3 \times 3 \times 2$ wurtzite unit cells (see Fig. 1). Since the ionicity of C is closer to that of N, than Al, it is expected that C will occupy predominantly N site in C-doped AlN. Indeed, theoretical investigations showed that in C-doped AlN the substitution of C at N site is preferred [38–42]. As mentioned above, first-principles calculations suggested that substitutional C or N at anion site can induce ferromagnetism in several oxides, sulfides and nitrides. In this work C atoms substitute N atoms in the supercells. The cell and atomic relaxation were carried out until the residual atomic forces were smaller than 0.05 eV/Å. The optimized lattice parameters of wurtzite AlN are $a = 3.126$ Å and $c = 5.011$ Å, in agreement with experimental values [50].

## 3. Results and discussion

The C-doped system $Al_{36}CN_{35}$, in which one N atom is substituted by one C in the supercell, is first investigated. Due to the larger atomic radius of C, the Al and N atoms around the C move outward and the displacement is not isotropic. After GGA and GGA + $U$ relaxation the C–Al bond length along the hexagonal c axis increases about 0.012 and 0.142 Å, and the other three C–Al bonds increase about 0.061 and 0.046 Å, respectively. As a result, the C–Al bond length along the c axis is smaller than that of other C–Al bonds for GGA relaxation, while it is opposite for GGA + $U$ relaxation. The total energy of spin polarized state calculated by GGA and GGA + $U$ is lower than that of non-spin polarized state by about 62.1 and 135.5 meV, respectively, which indicates that the ground state of C-doped AlN is magnetic. Both of the magnetic moments of the supercell calculated by GGA and GGA + $U$ are 1.0 $\mu_B$. Table 1 lists the magnetic moment distribution on the C, Al and N atoms in $Al_{36}CN_{35}$. It can be seen that the moment is mainly contributed by the substitutional C atom, its first neighboring Al atoms and some N atoms, among which the atomic moment of C is the biggest. The remaining moments are mainly located in the interstitial region around these atoms. Similar moment distributions have been found in C-doped GaN [19], ZnO [22], $TiO_2$ [24] and ZnS [25]. Figs. 2(a) and 2(b) show the space distribution of spin density in the relaxed supercell calculated by the GGA and GGA + $U$, respectively. The distribution in Fig. 2 reveals that the spin density is mainly localized on the vicinity of C atom and the first neighboring N atoms or out-of-plane first and fifth neighboring N atoms, with a small contribution from the first neighboring Al atoms. Different from GGA calculations, which show that the spin polarizations of Al and N atoms are mainly located on 3 first neighboring Al atoms in the hexagonal plane and 12 first neighboring N atoms, respectively, GGA + $U$ calculations show that the polarizations are mainly located on the first neighboring Al atom along c axis and 6 out-of-plane first neighboring and 6 fifth neighboring N atoms, and the polarizations of the out-of-plane first neighboring N are much larger than that of the fifth neighboring N atoms. Therefore, the $U$ correction obviously changes the magnetic moment distribution of Al and N atoms. Figs. 3(a) and 3(b) show the total density of states (DOS) of $Al_{36}CN_{35}$ and the partial DOS of 2p states of C atom, a first neighboring Al atom and a first neighboring N atom calculated by GGA and GGA + $U$, respectively. It can be seen that the C substitution induces the spin splitting impurity states above the top of the valence band. Similarly, the calculations by Bogusławski et al. [38,39] showed that substitutional C at N site creates impurity-induced levels above the top of the valence band. The impurity states are mostly formed by 2p states of the C and its first neighboring N atoms or out-of-plane first and fifth neighboring N atoms, whereas 2p states of first neighboring Al atoms also provide small contribution. This indicates that all of the magnetic moment comes from 2p orbitals, in which a majority of the moment comes from partially filled 2p orbitals of C atom and its first neighboring N atoms or out-of-plane first neighboring and fifth neighboring N atoms. Comparing Figs. 3(a) and 3(b) one can see that Fermi level passes through the minority-spin impurity states for GGA calculation, while the $U$ correction obviously enlarges splitting between the occupied and unoccupied minority-spin 2p states of C, its first neighboring Al and the first and fifth neighboring N atoms, which consequently open a gap of about 0.5 eV between the occupied and unoccupied minority-spin impurity states. Accordingly, the $U$ correction transforms the ground state of C-doped AlN to an insulating state.

Next, the system $Al_{36}C_2N_{34}$, in which two N atoms are substituted by C in a supercell, is investigated to study the magnetic coupling between the moments induced by C doping. We consider six different C–C positions in the supercell, where the first C atom is fixed at site 0 and the second C occupies one of sites 1 to 6, as shown in Fig. 1. Hereafter, $Al_{36}C_2N_{34}$ systems with the six C–C positions are named configurations (0, 1), (0, 2), (0, 3), (0, 4), (0, 5) and (0, 6). For each configuration, the spin-polarized GGA and GGA + $U$ calculations were performed, considering ferromagnetic (FM) and antiferromagnetic (AFM) coupling of the moments induced by C doping, respectively. The energy difference between FM and AFM states for each configuration, $\Delta E_m = E_{FM} - E_{AFM}$, is listed in Table 2. For the magnetic ground state of each configura-

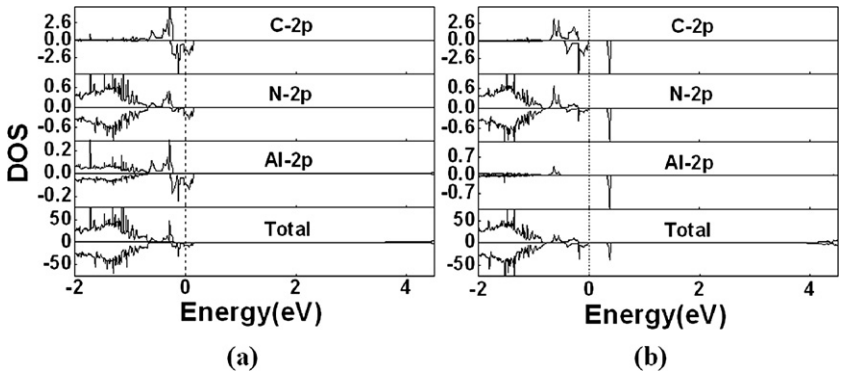


**Fig. 3.** Total and partial DOS of $Al_{36}CN_{35}$ calculated by GGA (a) and GGA + $U$ (b). The Fermi energy is indicated by the dashed vertical line.

**Table 2**
The relaxation C–C distance $d$ in ground state, the relative energy $\Delta E$, the energy difference $\Delta E_m$, and the magnetic moment of each C atom ($M_C$) and the supercell ($M_S$) in ground state.

| | Configuration $(0, i)$ | $d$ (Å) | $\Delta E$ (meV) | $\Delta E_m$ (meV) | $M_C$ ($\mu_B$) | $M_S$ ($\mu_B$) |
|---|---|---|---|---|---|---|
| GGA | (0, 1) | 4.373 | 78.7 | −25.9 | 0.276 | 2.0 |
| | (0, 2) | 4.415 | 68.4 | −23.4 | 0.280 | 2.0 |
| | (0, 3) | 5.415 | 72.2 | −18.5 | 0.272 | 2.0 |
| | (0, 4) | 5.910 | 0 | −21.2 | 0.287 | 2.0 |
| | (0, 5) | 5.910 | 0 | −21.2 | 0.287 | 2.0 |
| | (0, 6) | 7.360 | 94.3 | −9.5 | 0.274 | 2.0 |
| GGA + $U$ | (0, 1) | 4.367 | 118.5 | −12.0 | 0.290 | 2.0 |
| | (0, 2) | 4.393 | 104.3 | −27.6 | 0.294 | 2.0 |
| | (0, 3) | 5.429 | 25.4 | 90.3 | 0.299 | 0.0 |
| | (0, 4) | 5.882 | 0 | −20.3 | 0.310 | 2.0 |
| | (0, 5) | 5.882 | 0 | −20.3 | 0.310 | 2.0 |
| | (0, 6) | 7.378 | 141.6 | −4.8 | 0.283 | 2.0 |

tion, the relaxed C–C distance, relative energy $\Delta E$ with respect to the energy of the configuration $(0, 4)$, and the magnetic moment of each C atom and the supercell are also listed in Table 2. It can be seen that among all configurations, the configurations $(0, 4)$ and $(0, 5)$ are most stable for GGA and GGA + $U$ calculations. All $\Delta E_m$ calculated by GGA are negative, which indicates that the ground state is FM for all configurations. In contrast with the GGA calculations, $\Delta E_m$ for configuration $(0, 3)$ calculated by GGA + $U$ is a large positive value, meaning that the $U$ correction causes a transition of magnetic coupling from FM to strong AFM. Moreover, the $U$ correction significantly reduces FM coupling for configurations $(0, 1)$ and $(0, 6)$, while relative strong FM coupling for other three configurations are almost the same as those by GGA. Interestingly, both GGA and GGA + $U$ calculations show that among all configurations, the most stable configurations $(0, 4)$ and $(0, 5)$ have the largest magnetic moment of C atom and large negative $\Delta E_m$. This suggests that ferromagnetism is possible in C-doped AlN. Similar to the DOS of $Al_{36}CN_{35}$, the DOS of configurations $(0, 4)$ and $(0, 5)$ in FM state calculated by GGA and GGA + $U$ reveal that substitutional C atoms at N sites create the spin splitting impurity states above the top of the valence band and the $U$ correction opens a gap between the occupied and unoccupied minority-spin impurity states. Moreover, both GGA and GGA + $U$ calculations for all configurations show that the magnetic moment induced by each C dopant and corresponding moment distribution are nearly consistent with those in the cases of single C atom substitution in a supercell.

It has been known that standard LSDA and GGA are unable to predict correct Jahn–Teller-like structural distortion and underestimate the localization of anion-2p electrons [32,33,51]. As a consequence, in some cases a magnetic ground state is still predicted, but the spatial distribution of magnetic moment is inaccurate. This typically leads to a metallic or half-metallic ground state. Similar to the calculated results in monoxides by Pardo et al. [32], using a range of values of $U$ up to 5.6 eV, our calculations show that, for values of $U$ bigger than $\sim 2.7$ eV, the $U$ correction is able to modify the spatial distribution of magnetic moment and restore the correct energy splitting between occupied and unoccupied states via an enhanced localization of the 2p electrons responsible for the magnetism and the correct Jahn–Teller-like structural distortion.

The stabilization of FM state for C-doped AlN can be understood from the phenomenological two band coupling model [22,52,53]. In the FM configuration, the p states with the same spin can couple with each other, forming bonding and antibonding states for each spin channel. Partial occupation of the spin-down p states can stabilize the FM state through the energy gained from the filling of the lower spin-down bonding states, as shown in Fig. 4(a). The AFM state is stabilized by the super-exchange interaction between the fully occupied majority-spin state at the one site and the partially occupied minority-spin state at the other site. The AFM super-exchange interaction is smaller than FM coupling when the exchange splitting between the majority and minority spin p states is not zero [53], so the energy gain for the FM state is usually larger than that for AFM state, which indicates that the FM state for system is more stable. This model is confirmed by the DOS shown in Figs. 4(c) and 4(d), where indeed, both overall shape of calculated C-2p partial DOS by GGA and the corresponding occupation for the FM and AFM state agree with those predicted from the model shown in Figs. 4(a) and 4(b), respectively. Similarly, except a small gap between the occupied and unoccupied C-2p states, calculated C-2p partial DOS of configuration $(0, 4)$ by GGA + $U$ and the corresponding occupation for the FM and AFM state nearly agree with those predicted from the model.

## 4. Conclusions

In summary, a substitutional C dopant in AlN introduces magnetic moment of 1.0 $\mu_B$, which comes from the partially occupied 2p orbitals of C atom, its first neighboring Al and the first neighboring N atoms or out-of-plane first and fifth neighboring N atoms. The $U$ correction for the anion-2p states obviously changes the magnetic moment distribution of Al and N atoms and causes a transition of the ground state of C-doped AlN from metallic to insulating state, which indicates that the $U$ correction for the anion-2p states is essential for the correct description of the magnetism in C-doped AlN. The FM state is the stable ground state for C-doped AlN. Partial DOS of 2p states of C atom and the corresponding occupations show that the long-range FM coupling between the magnetic moments induced by C doping can be understood from the band coupling model.

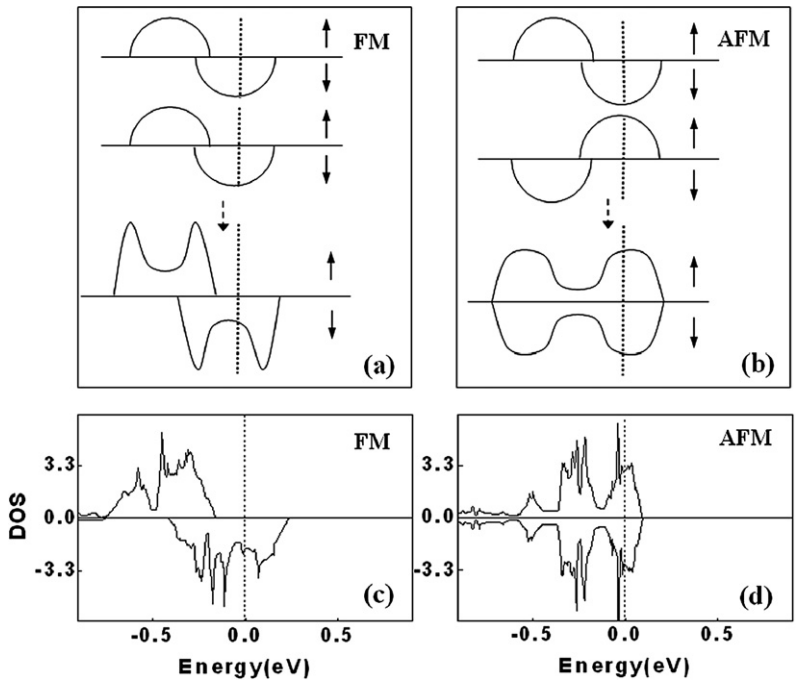


**Fig. 4.** Schematic diagram of the p states coupling between them in FM (a) and AFM (b) states. The Fermi energy is indicated by the dashed vertical line. The upper side shows the DOS for two isolated C defects, and underside is the final state after the coupling for the whole system. C-2p partial DOS of FM (c) and AFM (d) state for configuration $(0, 4)$ calculated by GGA.

## Acknowledgements

This work was supported by Specialized Research fund for the Doctoral Program of Higher Education (No. 200801830010) and the National Fund for Fostering Talents of basic Science (Grant No. J0730311).

## References

[1] K. Ueda, H. Tabata, T. Kawai, Appl. Phys. Lett. 79 (2001) 988.
[2] Y. Matsumoto, M. Murakami, T. Shono, T. Hasegawa, T. Fukumura, M. Kawasaki, P. Ahmet, T. Chikyow, S. Koshihara, H. Koinuma, Science 291 (2001) 854.
[3] S.B. Ogale, R.J. Choudhary, J.P. Buban, S.E. Lofland, S.R. Shinde, S.N. Kale, V.N. Kulkarni, J. Higgins, C. Lanci, J.R. Simpson, N.D. Browning, S. Das Sarma, H.D. Drew, R.L. Greene, T. Venkatesan, Phys. Rev. Lett. 91 (2003) 077205.
[4] J. Philip, N. Theodoropoulou, G. Berera, J.S. Moodera, B. Satpati, Appl. Phys. Lett. 85 (2004) 777.
[5] R.M. Frazier, G.T. Thaler, J.Y. Leifer, J.K. Hite, B.P. Gila, C.R. Abernathy, S.J. Pearton, Appl. Phys. Lett. 86 (2005) 052101.
[6] H. Hori, S. Sonada, T. Sasaki, Y. Yamamoto, S. Shimizu, K. Suga, K. Kindo, Physica B 324 (2002) 142.
[7] J.H. Park, M.G. Kim, H.M. Jang, S. Ryu, Y.M. Kim, Appl. Phys. Lett. 84 (2004) 1338.
[8] T.C. Kaspar, T. Droubay, S.M. Heald, M.H. Engelhard, P. Nachimuthu, S.A. Chambers, Phys. Rev. B 77 (2008) 201303(R).
[9] S. Zhou, K. Potzger, J. von Borany, R. Grotzschel, W. Skorupa, M. Helm, J. Fassbender, Phys. Rev. B 77 (2008) 035209.
[10] S.Q. Zhou, Q.Y. Xu, K. Potzger, G. Talut, R. Grotzschel, J. Fassbender, M. Vinnichenko, J. Grenzer, M. Helm, H. Hochmuth, M. Lorenz, M. Grudmann, H. Schmidt, Appl. Phys. Lett. 93 (2008) 232507.
[11] C.F. Yu, T.J. Lin, S.J. Sun, H. Chou, J. Phys. D: Appl. Phys. 40 (2007) 6497.
[12] C.F. Yu, S.H. Chen, S.J. Sun, H. Chou, J. Phys. D: Appl. Phys. 42 (2009) 035001.
[13] J.B. Yi, L. Shen, H. Pan, L.H. Van, S. Thongmee, J.F. Hu, Y.W. Ma, J. Ding, Y.P. Feng, J. Appl. Phys. 105 (2009) 07C513.
[14] T.S. Herng, S.P. Lau, C.S. Wei, L. Wang, B.C. Zhao, M. Tanemura, Y. Akaike, Appl. Phys. Lett. 95 (2009) 133103.
[15] T.S. Herng, S.P. Lau, L. Wang, B.C. Zhao, S.F. Yu, M. Tanemura, A. Akaike, K.S. Teng, Appl. Phys. Lett. 95 (2009) 012505.
[16] M.M. Cruz, R.C. da Silva, N. Franco, M. Godinho, J. Phys.: Condens. Matter 21 (2009) 206002.
[17] X.J. Ye, W. Zhong, M.H. Xu, X.S. Qi, C.T. Au, Y.W. Du, Phys. Lett. A 373 (2009) 3684.
[18] H. Pan, J.B. Yi, L. Shen, R.Q. Wu, J.H. Yang, J.Y. Lin, Y.P. Feng, J. Ding, L.H. Van, J.H. Yin, Phys. Rev. Lett. 99 (2007) 127201.
[19] L. Yu, Z.Y. Wang, M. Guo, D.H. Liu, Y. Dai, B.B. Huang, Chem. Phys. Lett. 487 (2010) 251.
[20] B.J. Nagare, S. Chacko, D.G. Kanhere, J. Phys. Chem. A 114 (2010) 2689.
[21] M. Pesci, F. Gallino, C. Di Valentin, G. Pacchioni, J. Phys. Chem. C 114 (2010) 1350.
[22] H.W. Peng, H.J. Xiang, S.H. Wei, S.S. Li, J.B. Xia, J.B. Li, Phys. Rev. Lett. 102 (2009) 017201.
[23] L. Shen, R.Q. Wu, H. Pan, G.W. Peng, M. Yang, Z.D. Sha, Y.P. Feng, Phys. Rev. B 78 (2008) 073306.
[24] K.S. Yang, Y. Dai, B.B. Huang, M.H. Whangbo, Appl. Phys. Lett. 93 (2008) 132507.
[25] S.W. Fan, K.L. Yao, Z.L. Liu, Appl. Phys. Lett. 94 (2009) 152506.
[26] H. Pan, Y.P. Feng, Q.Y. Wu, Z.G. Huang, J. Lin, Phys. Rev. B 77 (2008) 125211.
[27] J.G. Tao, L.X. Guan, J.S. Pan, C.H.A. Huan, L. Wang, J.L. Kuo, Z. Zhang, J.W. Chai, S.J. Wang, Appl. Phys. Lett. 95 (2009) 062505.
[28] L.X. Guan, J.G. Tao, C.H.A. Huan, J.L. Kuo, L. Wang, Appl. Phys. Lett. 95 (2009) 012509.
[29] R. Long, N.J. English, Phys. Lett. A 374 (2009) 319.
[30] K. Li, Y. Yan, H.X. Wang, X.T. Liu, Y.S. Mohammed, H.M. Jin, Phys. Lett. A 374 (2010) 319.
[31] I.S. Elfimov, A. Rusydi, S.I. Csiszar, Z. Hu, H.H. Hsieh, H.J. Lin, C.T. Chen, R. Liang, G.A. Sawatzky, Phys. Rev. Lett. 98 (2007) 137202.
[32] V. Pardo, W.E. Pickett, Phys. Rev. B 78 (2008) 134427.
[33] A. Droghetti, C.D. Pemmaraju, S. Sanvito, Phys. Rev. B 78 (2008) 140404(R).
[34] K.S. Yang, R.Q. Wu, L. Shen, Y.P. Feng, Y. Dai, B.B. Huang, Phys. Rev. B 81 (2010) 125211.
[35] F.Y. Ran, M. Subramanian, M. Tanemura, Y. Hayashi, T. Hihara, Appl. Phys. Lett. 95 (2009) 112111.
[36] X.H. Ji, S.P. Lau, S.F. Yu, H.Y. Yang, T.S. Herng, J.S. Chen, Nanotechnology 18 (2007) 105601.
[37] W.W. Lei, D. Liu, P.W. Zhu, X.H. Chen, Q. Zhao, G.H. Wen, Q.L. Cui, G.T. Zou, Appl. Phys. Lett. 95 (2009) 162501.
[38] P. Bogusławski, E.L. Briggs, J. Bernholc, Appl. Phys. Lett. 69 (1996) 233.
[39] P. Bogusławski, J. Bernholc, Phys. Rev. B 56 (1997) 9496.
[40] C.H. Park, D.J. Chadi, Phys. Rev. B 55 (1997) 12995.
[41] I. Gorczyca, A. Svane, N.E. Christensen, Phys. Rev. B 60 (1999) 8147.
[42] L.E. Ramos, J. Furthmüller, L.M.R. Scolfaro, J.R. Leite, F. Bechstedt, Phys. Rev. B 66 (2002) 075209.
[43] G. Kresse, J. Hafner, Phys. Rev. B 47 (1993) 558;
G. Kresse, J. Hafner, Phys. Rev. B 49 (1994) 14251.
[44] G. Kresse, J. Furthmüller, Comput. Mat. Sci. 6 (1996) 15;
G. Kresse, J. Furthmüller, Phys. Rev. B 54 (1996) 11169.
[45] J.P. Perdew, K. Burke, M. Ernzerhof, Phys. Rev. Lett. 77 (1996) 3865.

[46] V.I. Anisimov, J. Zaanen, O.K. Andersen, Phys. Rev. B 44 (1991) 943;
V.I. Anisimov, I.V. Solovyev, M.A. Korotin, M.T. Czyzyk, G.A. Sawatzky, Phys. Rev. B 48 (1993) 16929.
[47] J. Ghijsen, L.H. Tjeng, J. van Elp, H. Eskes, J. Westerink, G.A. Sawatzky, M.T. Czyzyk, Phys. Rev. B 38 (1988) 11322.
[48] L.H. Tjeng, et al., Strong Correlation and Superconductivity, in: H. Fukuyama, S. Maekawa, A.P. Malozemoff (Eds.), Springer Series in Solid-State Sciences, vol. 89, Springer-Verlag, Berlin, 1989, p. 85.
[49] L.H. Tjeng, PhD thesis, University of Groningen, 1990.
[50] S. Strite, H. Morkoc, J. Vac. Sci. Technol. B 10 (1992) 1237.
[51] J.A. Chan, S. Lany, A. Zunger, Phys. Rev. Lett. 103 (2009) 016404.
[52] A. Walsh, J.L.F. Da Silva, S.H. Wei, Phys. Rev. Lett. 100 (2008) 256401.
[53] G.M. Dalpian, S.H. Wei, X.G. Gong, A.J.R. Da Silva, A. Fazzio, Solid State Commun. 138 (2006) 353.